

Excellent BODIPY Dye Containing Dimesitylboryl Groups as PeT-Based Fluorescent Probes for Fluoride

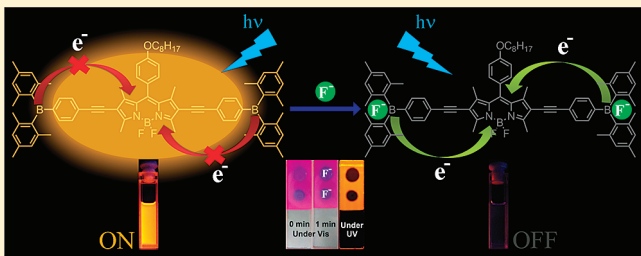
Huibin Sun,^{†,‡} Xiaochen Dong,^{†,‡} Shujuan Liu,[†] Qiang Zhao,^{*,†} Xin Mou,[†] Hui Ying Yang,^{*,§} and Wei Huang^{*,†}

[†]Key Laboratory for Organic Electronics and Information Displays (KLOEID) and Institute of Advanced Materials (IAM), Nanjing University of Posts and Telecommunications (NUPT), 9 Wenyuan Road, Nanjing 210046, People's Republic of China

[§]Pillar of Engineering Product Development, Singapore University of Technology and Design, Singapore 27923

Supporting Information

ABSTRACT: A highly selective fluorescent probe BBDPB for F^- was realized on the basis of the boron-dipyrromethene (BODIPY) dye containing two dimesitylboryl (Mes_2B) moieties. The fluorophore displays highly efficient orange-red fluorescence with an emission peak of 602 nm and quantum efficiency (Φ) of 0.65 in dichloromethane solution. Signaling changes were observed through UV/vis absorption and photoluminescence spectra. Obvious spectral changes in absorption and fluorescent emission bands were detected after adding F^- in company with an obvious solution color change from pink to deep blue. The effects of F^- on the electronic structure of BBDPB were studied in detail by performing theoretical calculations using the Gaussian 03 package. According to the theoretical calculation and contrast experiments, the binding of Mes_2B moieties with F^- would give rise to nonradiative photoinduced-electron-transfer (PeT) deactivation from Mes_2B moieties to BODIPY core and then quench the fluorescence. To implement this approach, an excellent solid-film sensing device was designed by doping BBDPB in polymethylmethacrylate (PMMA).



1. INTRODUCTION

Anions are ubiquitous throughout biological systems and play a fundamental role in a wide range of chemical and biological processes.^{1–5} One of them is the small fluoride anions (F^-), which commonly exist in drinking water, toothpaste, and osteoporosis drugs.⁶ Despite the importance of fluoride anions in the treatment of osteoporosis and dental care, the quantifying and sensing F^- remain challenging. Currently, intensive investigations have been focused on the development of fluorescent probes for F^- , which can realize fluorescent detection with high sensitivity and short response time.^{7–9} Because the fluorescent method can detect F^- by the “naked eye” and provide both qualitative and quantitative information with simple equipment, it is considered as a viable F^- detection technology at low cost and low energy consumption.^{10–12}

Boron-dipyrromethene (BODIPY) dyes are a class of well-known fluorophores with widespread applications as fluorescent probes because of their outstanding optical properties, such as sharp and intense absorption with high molar absorption coefficients, high fluorescence quantum efficiencies, and robustness against light and chemical.^{13–15} Thus, it is critical to develop suitable BODIPY dyes for F^- probes, especially for realizing naked-eye detection with simple and low-cost operation. Three-coordinate organoboron compounds containing dimesitylboryl (Mes_2B) moieties have recently emerged as a new class of materials for various optoelectronic applications due to their unique ability

to accept electrons through the empty p_{π} orbital on the boron center.^{16–21} The empty p_{π} orbital makes organoboron compounds the Lewis acid, which can be used as an effective receptor for strong Lewis bases, such as F^- .^{22–25} It is highly desirable to develop efficient fluorescent probes for F^- based on the BODIPY dye modified with Mes_2B moieties.

Photoinduced electron transfer (PeT) is a fundamental mechanism responsible for the fluorescence quenching or enhancement of fluorophores when photoactive materials interact with light.^{26–29} The PeT process is an effective strategy to construct fluorescent probes and has been widely utilized for spectroscopic sensing of metal ions.^{30–34} It has been proven that the chemical structures of pendant group can strongly affect the photophysical properties of BODIPY dyes. The applications of the PeT mechanism in fluorescent probes based on BODIPY dyes have been reported by a few research groups.^{35–40} Nevertheless, the F^- ion detection based on the technique has not been realized.

Herein, we reported a fluorophore based on a BODIPY dye (BBDPB) linked with two Mes_2B moieties as pendant groups (see Scheme 1), which was synthesized by the Sonogashira coupling reaction between the diiodo-substituted BODIPY 2 and the (4-ethynylphenyl) dimesitylboratione 4 (see Scheme 2). Furthermore,

Received: July 6, 2011

Revised: September 2, 2011

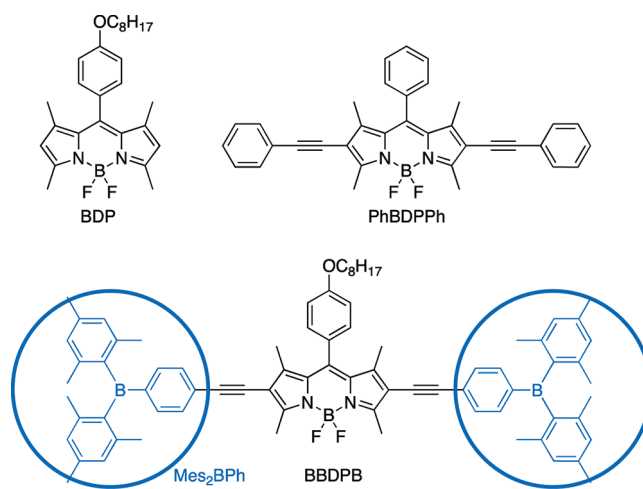
Published: September 06, 2011

the F-induced electron-donating ability change in pendant groups has been attributed to the PeT process. Because the pendant groups contain specific receptors (Mes_2B moieties) for fluoride ions, we reason that the presence of fluoride ions can give rise to the elevation of the energy level of the highest occupied molecular orbital (HOMO) located at Mes_2B moieties and facilitate the PeT process from Mes_2B moieties to BODIPY core and then lead to dramatic changes in the photophysical properties of fluorophore. As a result, a turn-off type fluorescent probe for fluoride ions can be realized successfully.

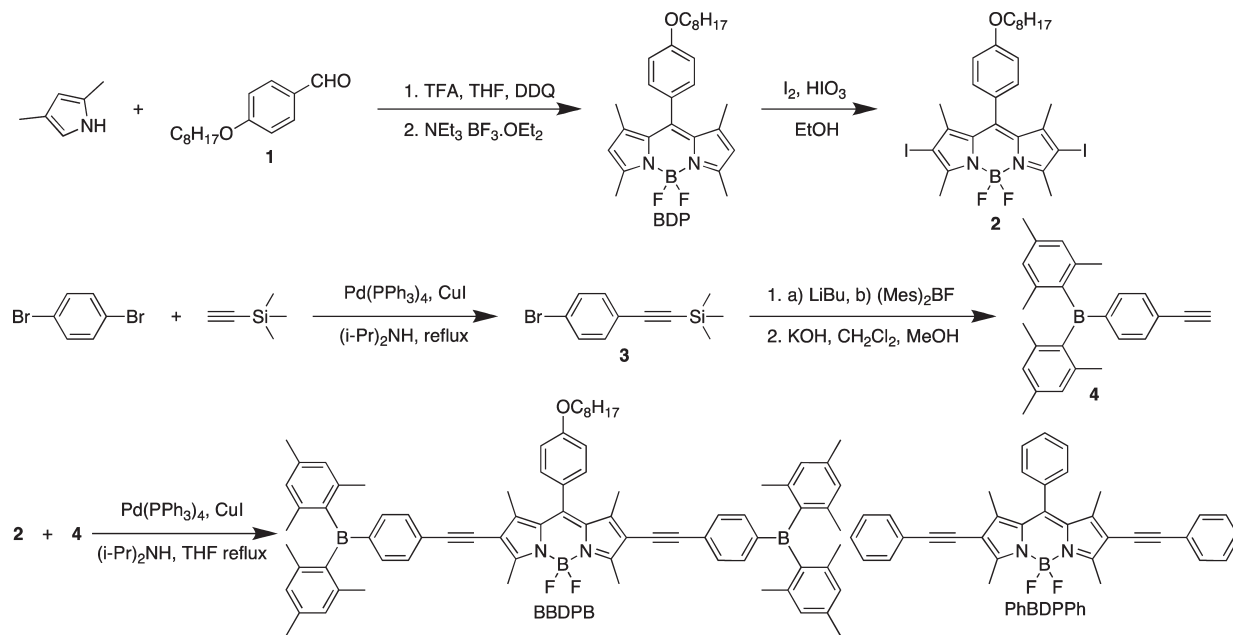
2. EXPERIMENTAL SECTION

2.1. General Procedures. All the materials listed below were of research grade or spectrograde in the highest purity and commercially available from Alfa or Acros Organics. Dichloromethane (CH_2Cl_2), diisopropylamine ($(i\text{-Pr})_2\text{NH}$), tetrahydrofuran (THF),

Scheme 1. Molecular Structures of Compounds BDP, PhBDPPh,⁴¹ and BBDBPB



Scheme 2. Synthetic Procedure for the Compounds



and acetonitrile (CH_3CN) were purified before use. The reactions were all performed in a nitrogen atmosphere. Chromatography and thin-layer chromatography (TLC) were performed on silica (300–400 mesh). ^1H (400 MHz) and ^{13}C NMR (100 MHz) spectra were recorded at room temperature using trimethylsilane (TMS) as an internal standard on Bruker Ultra Shield Plus 400 MHz instrument. The mass spectra were obtained on a Brukerautoflex MALDI-TOF/TOF mass spectrometer. The UV/vis absorption spectra were recorded on a Shimadzu UV-3600 UV/vis-NIR spectrophotometer. The photoluminescence spectra were measured using a RF-5301PC spectrofluorophotometer.

2.2. Synthesis of Probe. *4-(Octyloxy)benzaldehyde (1).* When 120 mL of degassed acetone was added to a 500 mL three-neck round-bottom flask containing 4-hydroxylbenzaldehyde (5 g, 41 mmol), 1-bromoocetane (9.8 g, 51.25 mmol), and K_2CO_3 (20 g, 144 mmol) under a nitrogen atmosphere, the mixture was stirred overnight in reflux conditions. After completing the reaction, which was monitored by TLC, the reaction mixture was concentrated under reduced pressure. The residue was dissolved in 50 mL of ethyl acetate and washed twice with water and brine. The organic layer was collected, dried over anhydrous Na_2CO_3 , and concentrated under reduced pressure. The resulting crude product was purified by silica gel column chromatography using petroleum ether/ethyl acetate (30/1, v/v) to obtain white solid (6.5 g, 67.6%). ^1H NMR (400 MHz, CDCl_3): δ = 9.84 (s, 1H), 7.79 (d, J = 8.6 Hz, 2H), 6.95 (d, J = 8.6 Hz, 2H), 4.0 (m, 2H), 1.78 (m, 2H), 1.48–1.21 (m, 10H), 0.86 (m, 3H); ^{13}C NMR (100 MHz, CDCl_3): δ = 190.66, 164.25, 131.93, 129.74, 114.71, 68.39, 31.79, 29.31, 29.21, 29.05, 25.96, 22.65, 14.08 ppm.

4,4-Difluoro-8-(4-octyloxyphenyl)-1,3,5,7-tetramethyl-4-bora-3a,4a-diaza-s-indacene (BDP). *4-(Octyloxy)benzaldehyde* (0.703 g, 3.0 mmol) and 2,4-dimethylpyrrole (0.63 g, 6.6 mmol) were dissolved in dry THF (90 mL) under a nitrogen atmosphere. Three drops of trifluoroacetic acid (TFA; about 0.2 mL) were added, and the mixture was stirred at room temperature overnight. After TLC monitoring showed complete disappearance of the 4-(octyloxy)benzaldehyde, a solution of 2,3-dichloro-5,6-dicyano-1,4-benzoquinone

(DDQ; 0.68 g, 3.0 mmol) in anhydrous THF (120 mL) was added. This mixture was further stirred for 3 h, then 18 mL of triethylamine (Et_3N) and 18 mL of $\text{BF}_3 \cdot \text{OEt}_2$ were successively added. After reacting overnight, the reaction mixture was washed thoroughly with water and brine, dried over anhydrous Na_2CO_3 , filtered, and evaporated under vacuum. The crude compound was purified by silica gel column chromatography (eluent: petroleum ether/ethyl acetate, from first 30:1 to final 10:1, increasing the polarity of the solvent) to give a shiny orange powder (0.85 g, 62.6%). ^1H NMR (400 MHz, CDCl_3): δ = 7.15 (d, J = 8.6 Hz, 2H), 6.99 (d, J = 8.6 Hz, 2H), 5.97 (s, 2H), 4.00 (m, 2H), 2.55 (s, 6H), 1.82 (m, 2H), 1.46–1.53 (m, 2H), 1.43 (s, 6H), 1.26–1.40 (m, 8H), 0.90 (m, 3H); ^{13}C NMR (100 MHz, CDCl_3): δ = 159.73, 155.20, 143.19, 142.02, 131.87, 129.14, 126.80, 121.07, 115.07, 77.36, 77.04, 76.72, 68.18, 31.83, 29.42, 29.27, 29.25, 26.08, 22.68, 14.59, 14.12 ppm.

4,4-Difluoro-8-(4-octyloxyphenyl)-2,6-diiodo-1,3,5,7-tetramethyl-4-bora-3a,4a-diaza-s-indacene (2). BDP (452.4 mg, 1 mmol) and iodine (583.7 mg, 2.3 mmol) were added to a flask containing 30 mL of ethanol (EtOH), and then iodic acid (323 mg, 2.3 mmol) dissolved in 1 mL of water was added to the solution. The reaction mixture was stirred at 60 °C and monitored by TLC. When all the starting materials have been consumed, saturated $\text{Na}_2\text{S}_2\text{O}_3$ solution in water was added and the product was extracted into CH_2Cl_2 . The solvent was evaporated and the residue was purified by neutral alumina column chromatography using petroleum ether/ethyl acetate (40/1, v/v) to obtain a wine solid (675 mg, 96%). ^1H NMR (400 MHz, CDCl_3): δ = 7.11 (d, J = 8.7 Hz, 2H), 7.02 (d, J = 8.7 Hz, 2H), 4.02 (t, J = 6.6 Hz, 2H), 4.02 (m, 2H), 2.64 (s, 6H), 1.92–1.74 (m, 1H), 1.54–1.46 (m, 2H), 1.45 (s, 6H), 1.41–1.27 (m, 8H), 0.90 (m, 3H); ^{13}C NMR (100 MHz, CDCl_3): δ = 159.73, 155.20, 143.19, 142.02, 131.87, 129.14, 126.80, 121.07, 115.07, 68.18, 31.83, 29.42, 29.27, 29.25, 26.08, 22.68, 14.59, 14.12.

((4-Bromophenyl)ethynyl)trimethylsilane (3). 1,4-Dibromo-benzene (2.0 g, 8.48 mmol) and $\text{Pd}(\text{PPh}_3)_4$ (98 mg, 0.085 mmol) were added to a three-neck round-bottom flask under a nitrogen atmosphere. When 55 mL of anhydrous degassed diisopropylamine and trimethylsilylacetylene were added to the flask, the mixture was stirred under reflux for 4 h. After the completion of the reagent, which was monitored by TLC, the reaction mixture was concentrated and dissolved in CH_2Cl_2 and washed twice with water and saturated saline solution. The organic layer was collected, dried over anhydrous Na_2CO_3 , and concentrated under reduced pressure. The product was purified by silica gel column chromatography using petroleum ether to yield a white solid (600 mg, 28%). ^1H NMR (400 MHz, CDCl_3): δ = 7.43 (d, J = 8.4 Hz, 2H), 7.32 (d, J = 8.4 Hz, 2H), 0.25 (s, 9H); ^{13}C NMR (100 MHz, CDCl_3): δ = 133.34, 131.43, 122.72, 122.04, 103.83, 95.53, –0.14.

((4-(Dimesitylboryl)phenyl)ethynyl)trimethylsilane. To a solution of 3 (506.4 mg 2 mmol) in THF (10 mL) was added a hexane solution of *n*-BuLi (1.6 M, 1.38 mL, 2.2 mmol) at –78 °C, and the mixture was stirred for 1 h at this temperature. A solution of dimesitylboron fluoride (0.66 g, 2.2 mmol) in THF (2 mL) was then added. The reaction mixture was stirred for another hour at –78 °C, then allowed to slowly reach room temperature and stirred overnight. The solvents were removed under reduced pressure. The residue was subjected to column chromatography on silica gel using petroleum ether to afford white crystal 397 mg in yield of 47%. ^1H NMR

(400 MHz, CDCl_3): δ = 7.44 (s, 4H), 6.82 (s, 4H), 2.31 (s, 6H), 1.98 (s, 12H), 0.26 (s, 9H); ^{13}C NMR (100 MHz, CDCl_3): δ = 140.87, 140.85, 138.87, 135.90, 131.44, 128.23, 128.11, 126.25, 105.26, 96.51, 23.41, 21.24, –0.07.

(4-Ethynylphenyl)dimesitylborane (4). ((4-(Dimesitylboryl)-phenyl)ethynyl)trimethylsilane (126.7 mg, 0.3 mmol) was dissolved in 5 mL CH_2Cl_2 under a nitrogen atmosphere. When 5 mL of methanol solution of potassium hydroxide (84.2 mg, 1.5 mmol) was successively added, the mixture was stirred for 30 min at room temperature. Then, the reaction finished by extracting with water and dichloromethane three times. The organic layer was dried with anhydrous Na_2CO_3 and evaporated under reduced pressure. The product was purified by silica gel column chromatography using petroleum ether/ethyl acetate (60:1, v/v) to yield white crystal (85 mg, 81%). ^1H NMR (400 MHz, CDCl_3): δ = 7.47 (s, 4H), 6.83 (s, 4H), 3.18 (s, 1H), 2.31 (s, 6H), 1.99 (s, 12H), 0.26 (s, 9H); ^{13}C NMR (100 MHz, CDCl_3): δ = 140.83, 138.94, 135.93, 131.61, 128.26, 125.26, 83.90, 79.01, 23.44, 21.25.

4,4-Difluoro-8-(4-octyloxyphenyl)-2,6-di((4-(dimesitylboryl)-phenyl)ethynyl)-1,3,5,7-tetramethyl-4-bora-3a,4a-diaza-s-indacene (BBDPB). A flask charged with 10 mL of freshly distilled THF and 5 mL (*i*-Pr)₂NH was purged with N_2 for 15 min, and 4 (87.6 mg, 0.25 mmol), 2 (49.6 mg, 0.1 mmol), Pd(PPh_3)₄ (26.4 mg, 0.025 mmol), and CuI (4.7 mg, 0.025 mmol) were added. After the solution was stirred for 12 h at 60 °C, the reaction mixture was evaporated under reduced pressure and the compound was purified over silica gel using petroleum ether/ethyl acetate (50/1, v/v) to yield 41 mg purple solid in 39% yield. ^1H NMR (400 MHz, CDCl_3): δ = 7.47 (d, J = 8.2 Hz, 4H), 7.41 (d, J = 8.2 Hz, 4H), 7.17 (d, J = 8.6 Hz, 2H), 7.04 (d, J = 8.7 Hz, 2H), 6.82 (s, 8H), 4.03 (m, 2H), 2.72 (s, 6H), 2.31 (s, 12H), 2.00 (s, 24H), 1.89–1.79 (m, 2H), 1.60 (s, 6H), 1.55–1.24 (m, 8H), 0.90 (s, 3H); ^{13}C NMR (100 MHz, CDCl_3): δ = 160.10, 158.46, 145.64, 144.39, 143.01, 141.53, 140.84, 138.83, 136.18, 131.78, 130.70, 129.06, 128.23, 126.75, 126.08, 115.93, 115.33, 96.95, 83.99, 77.35, 77.23, 77.03, 76.71, 68.27, 31.95, 31.83, 31.45, 30.20, 29.72, 29.68, 29.42, 29.38, 29.25, 26.07, 23.45, 22.71, 22.68, 21.24, 14.14, 14.13, 13.71, 1.04, 0.01; MS (MALDI-TOF) (*m/z*): 1148.850.

2.3. Quantum Yields. Quantum yields were calculated by comparing the integrated emission area of the corrected spectra to the area measured for Rhodamine B in ethanol when excited at 360 nm ($\Phi = 0.71$).⁴² The quantum yields for BDP and BBDPB were then calculated using eq 1, where F represents the area under the emission spectra for the standard and samples, η is the refractive index of the solvent, and Abs is the absorbance at the excitation wavelength selected for the standard and samples. Emission was integrated between 500 and 700 nm ($\lambda_{\text{ex}} = 360$ nm, 10^{-7} M, $\text{Abs}_{360} \approx 0.08$).

$$\Phi_{\text{fl}}^{\text{sample}} = \Phi_{\text{fl}}^{\text{standard}} \left(\frac{F^{\text{sample}}}{F^{\text{standard}}} \right) \left(\frac{\eta^{\text{sample}}}{\eta^{\text{standard}}} \right) \left(\frac{\text{Abs}^{\text{standard}}}{\text{Abs}^{\text{sample}}} \right) \quad (1)$$

2.4. Computational Methods. Orbital energies were calculated by using Gaussian 03 at B3LYP density functional theory (DFT).⁴³ The 6-31G (d) basis set was used to treat all atoms. To reduce the calculation time, all the alkyl chains were substituted by methoxyl. The Mes₂BPh fragment was modeled independent of the BODIPY fragment. The binding energy of the boron atoms with F[–] is obtained by counter-poise calculations. The binding energy, E_b , can be expressed by eq 2 according to the

reported method in literature:⁴⁴

$$E_b = E_{AB}(AB) - E_A^0(A) - E_B^0(B) + [E_A(A) - E_A(AB)] + [E_B(B) - E_B(AB)] \quad (2)$$

where $E_X(Y)$ is the energy of the subsystem (fragment) X calculated in the basis of unit Y , E^0 is the energy of the free fragments in their equilibrium geometries, and E is the energies of the fragments in their actual geometries within the AB complex. Herein, A, B, and AB represent BBDPB, F^- , and FBDPBF, respectively. The terms in the square brackets show the energy correction due to the change of basis set size when the different parts of the combined molecule approach one another.

2.5. Titration of BBDPB with F^- . Spectrophotometric titrations were performed on 2 μM solutions of BBDPB in CH_2Cl_2 . Typically, aliquots of fresh tetrabutylammonium fluoride (TBAF) in CH_3CN were added, and the UV/vis absorption and fluorescent spectra of the samples were recorded. The excitation wavelength was $\lambda_{\text{ex}} = 430$ nm, the excitation slit widths were set at 5.0 nm, and the emission slit widths were set at 3.0 nm, and the emission spectra were recorded every 5 min. Absorption and emission spectra were recorded sequentially until no further changes were observed. The stability constants for the binding of one and two fluoride ions to the BBDPB in CH_2Cl_2 were determined from the UV/vis absorption titrations, fitting the absorbance changes at several wavelengths to eq 3 by Matlab.⁴⁵

$$\Delta A = \frac{[H](K_1\Delta\varepsilon_{11}[F^-] + K_1K_2\Delta\varepsilon_{12}[F^-]^2)}{1 + K_1[F^-] + K_1K_2[F^-]^2} \quad (3)$$

2.6. Fluorescence Selectivity of BBDPB with Various Anions. Commercially available quaternary ammonium salts of other anions were used in these experiments. All the salts were prepared as stock CH_3CN solutions. A 7-fold excess of each of the anions was added to 2 μM solutions of BBDPB in CH_2Cl_2 . Fluorescence spectra were recorded after 5 min.

3. RESULTS AND DISCUSSION

3.1. Synthesis and Characterization of BBDPB. The target dye BBDPB was synthesized from the diiodo-substituted BODIPY 2 and the (4-ethynylphenyl)dimesitylborane 4 in 39% yield using palladium-catalyzed Sonogashira reaction (see Scheme 2). The precursor BDP was constructed by 2,4-dimethylpyrrole and 4-(octyloxy)benzaldehyde using literature procedures,⁴⁶ and the precursor compound 4 was obtained by the reaction of 3 with *n*-butyllithium, which converted it to a lithium salt, and then subsequently reacted with dimesitylboron fluoride to replace the fluoride. The target compound was characterized by ^1H NMR, ^{13}C NMR spectra and MALDI-TOF mass spectrometry.

3.2. Photophysical Properties. The UV/vis absorption and photoluminescent (PL) spectra of BDP and BBDPB are shown in Figure 1 and the photophysical properties are summarized in Table 1, which are also compared with the known dye PhBDPPh (see Scheme 1).⁴¹ Compound BBDPB features two major absorption bands at 356 and 576 nm in CH_2Cl_2 solution, which are assigned to the dominant $\pi-\text{p}_\pi$ (B) transition in the borane^{47,48} and the $S_0 \rightarrow S_1$ transition in the BODIPY core, respectively, and there is a shoulder at 420 nm observed, which can be assigned to the $S_0 \rightarrow S_2$ transition in the BODIPY core.⁴⁹ It can be seen that BBDPB displayed an orange-red emission in CH_2Cl_2 with a maximal emission wavelength at $\lambda = 602$ nm and a quantum efficiency of $\Phi = 0.65$. Compared with BDP, both absorption and

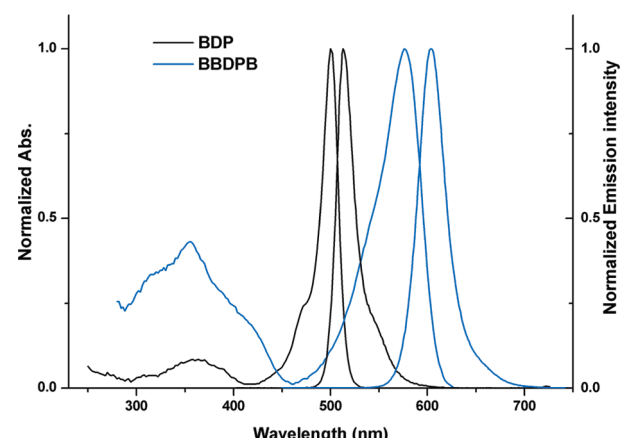


Figure 1. Normalized UV/vis absorption and PL spectra of BDP and BBDPB moieties in CH_2Cl_2 .

Table 1. Photophysical Data for BDP, PhBDPPh, and BBDPB

compound	λ_{abs} [nm] (log ε)	λ_{em} [nm]	Φ	τ [nm]
BDP	500 (4.97)	513	0.76 ^a	
PhBDPPh ⁴¹	561 (4.86)	594	0.82	
BBDPB	356 (4.80), 576 (5.16)	602, ^a 598, ^b 604 ^c	0.65 ^a	4.39, ^a 4.37, ^b 5.40 ^c

^a In CH_2Cl_2 . ^b In CH_3CN . ^c In hexane (see Supporting Information). Rhodamine B was used as the reference dye ($\Phi = 0.71$ in EtOH) for the measurement of Φ .⁴²

emission bands of BBDPB showed the evident red-shift of 76 nm due to the increase of conjugated length. In addition, the introduction of Mes₂B group also results in the red-shift in absorption and emission bands compared with PhBDPPh. The dependence of both the absorption and emission spectra of dye BBDPB on the solvent was studied in details. There was no significant change in the absorption and emission spectra in different solvents (Table 1), indicating no evident charge transfer state in BBDPB.

For a better understanding of the optical properties of BBDPB, theoretical calculations were performed using the Gaussian 03 package at the B3LYP level (Figure 2). The calculation results reveal that both the highest occupied molecular orbital and lowest unoccupied molecular orbital (LUMO) of BBDPB are mainly located at the BODIPY core, whereas the boron atom of Mes₂B unit contribute a little to the frontier orbital, which can explain why the introducing of Mes₂B unite just caused about 15 and 8 nm red-shift of the maximum absorption and emission peaks of BBDPB, respectively, compared with PhBDPPh.⁴¹ Meanwhile, according to the results of theoretical calculations and experiment, the excited state of BBDPB can be mainly assigned to $\pi \rightarrow \pi^*$ transition accompanied with little charge transfer (CT) state, which is responsible for its optical properties.

3.3. Optical Response of BBDPB to F^- . The response of BBDPB to F^- was investigated through UV/vis absorption and emission spectroscopic analysis. Figure 3 shows the changes in the absorption spectra of BBDPB upon the addition of F^- ions. The absorption at 356 nm decreased gradually and disappeared finally. This phenomenon reflects the vanishing of $\pi-\text{p}_\pi$ (B)

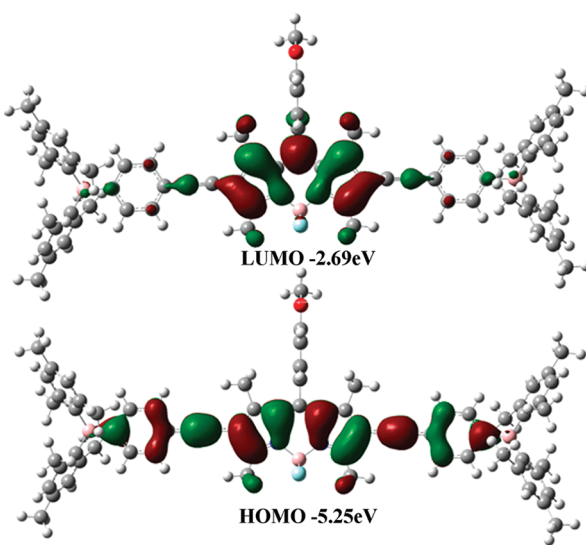


Figure 2. HOMO and LUMO distributions of BBDPB.

transition in the borane due to the binding of B with F^- . At the same time, the absorption at 576 nm also decreased gradually and was red-shifted to 589 nm. According to the frontier orbital distribution of BBDPB nearby Mes_2B unit shown in Figure 2, we can see that lobe size of the LUMO is considerably smaller than that of the HOMO, which leads to an expected destabilization of the HOMO through the introduction of electron-rich groups. Hence, the energy gap between the HOMO and LUMO is expected to decrease owing to the introduction of F^- . More importantly, the changes of absorption properties induce an evident change of solution color from pink to blue. This result indicates that BBDPB can serve as a sensitive “naked-eye” indicator for F^- (Figure 3). Using the UV-vis titration data, the binding constants (K_1 and K_2) of two three-coordinate boron atoms in BBDPB with F^- were determined to be 6.6×10^7 and $9.0 \times 10^4 \text{ M}^{-1}$, respectively (see Supporting Information), which are similar to the values reported previously for boryl-based fluorescent receptors.⁴⁵

The fluorescent emission spectroscopy is more sensitive toward small changes that affect the electronic properties of molecular receptors. The sensing ability of BBDPB toward F^- was also investigated by PL spectra. The variation in the PL spectra with 430 nm as the excitation wavelength is shown in Figure 4. Upon the addition of F^- ions to a solution of BBDPB in CH_2Cl_2 , the fluorescent emission intensity at 602 nm decreased gradually. After addition of approximately 6 equiv of F^- , the emission of BBDPB at 602 nm is completely quenched. This can be explained by utilizing the photoinduced electron transfer as the signaling mechanism. According to titration experiments, probe BBDPB can detect the F^- concentration of lower than $2 \times 10^{-7} \text{ M}$.

For a better understanding of the optical change after BBDPB binding with 2 equiv of F^- , theoretical calculations were also performed on F-BBDPB-F. Compared with BBDPB, the calculation results reveal that the HOMO of F-BBDPB-F is delocalized on the whole conjugated backbone from Mes_2B to BODIPY core and the LUMO is localized at the BODIPY core (Figure 5). At the same time, the energy gap between HOMO and LUMO decreased about 0.57 eV compared to BBDPB, which corresponds to the red-shift of the absorption in 576 nm after BBDPB binding with F^- . The significant distribution difference between HOMO and LUMO of F-BBDPB-F shows that there is partial electron transfer

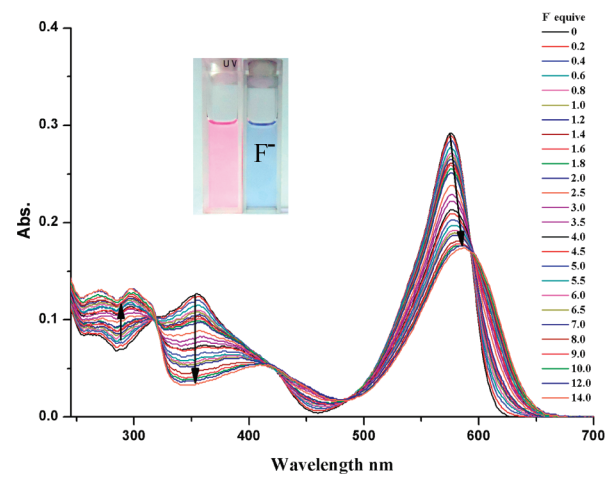


Figure 3. Change in UV/vis absorption spectra of BBDPB ($2.0 \mu\text{M}$) in CH_2Cl_2 with various amounts of F^- ions. Inset: solution color change upon addition of F^- (2 equiv).

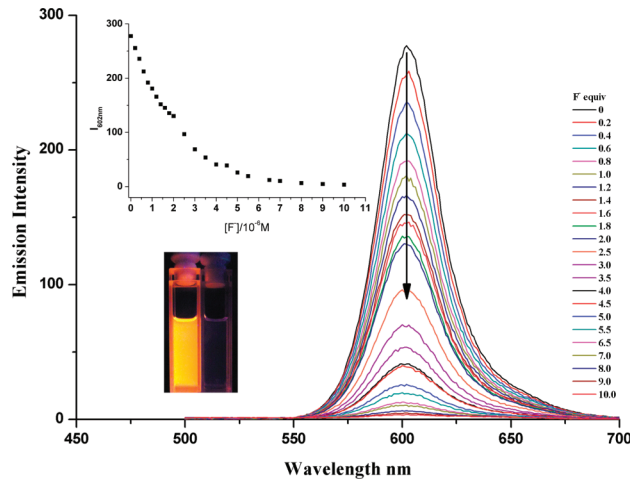


Figure 4. Change in the emission spectra of BBDPB ($2.0 \mu\text{M}$) in CH_2Cl_2 with various amounts of F^- ions excited at $\lambda = 430 \text{ nm}$. Inset: plot of $I_{602} \text{ nm}$ vs the concentration of F anions and observed emission color of BBDPB in CH_2Cl_2 ($2.0 \mu\text{M}$) in the absence (left) and presence (right) of F^- (4 equiv).

from two phenylborane-F moieties to BODIPY core. And this is likely related to the PeT process between the phenylborane-F moieties and BODIPY core, which quenches the fluorescence.

3.4. Mechanism of BBDPB in Sensing F^- . As mentioned above, three-coordinate organoboron as Lewis acid can bind with F^- . But there is another four-coordinate boron center in BODIPY core, which may also be disrupted by excessive F^- ^{50,51} as shown in Scheme 1. To demonstrate the binding of F^- with a three-coordinate boron atom (B1) rather than a four-coordinate boron atom (B2), the response of BDP without Mes_2BPh moieties to F^- was also measured. As shown in Figure 6, after addition of approximately 50 equiv F^- , the emission of BDP showed no significant change. Upon addition of 7 equiv F^- , however, the emission of BBDPB is completely quenched. This demonstrated that F^- is prior to binding with three-coordinate boron atoms in the measurement range of F^- concentration.

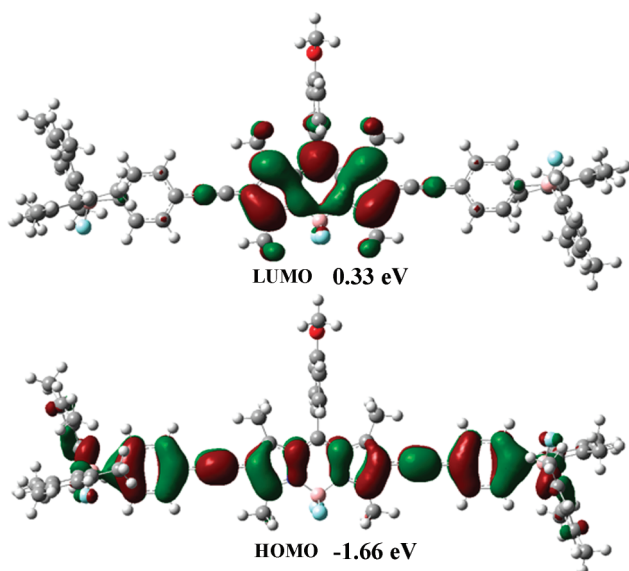


Figure 5. HOMO and LUMO distributions of F-BBDPB-F.

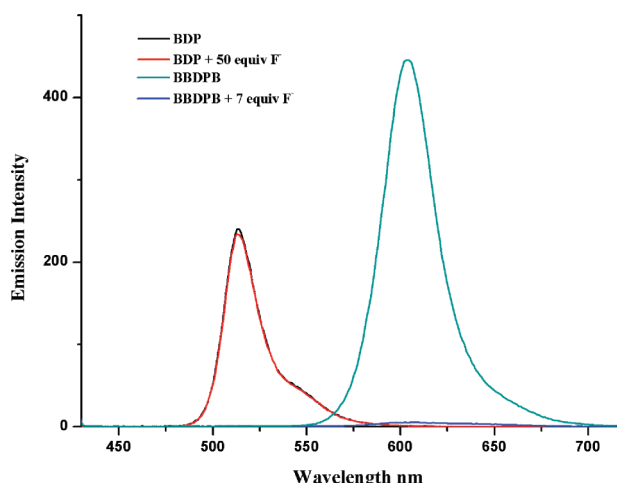


Figure 6. Optical responses of BDP and BBDPB to F^- under the same concentration ($2.0 \mu M$).

In addition, we have calculated the binding energy between the boron atoms and F^- in the two binding situation, respectively. The calculated binding energies are -115.57 kcal/mol for B1– F , and -57.91 kcal/mol for B2– F , respectively. According to the results of theoretical calculation, F^- is easier to bind with three-coordinate B1 than B2.

As we have mentioned before, the fluorescent probe for F^- is realized by the facilitated intramolecular PeT process due to the introducing of F^- . To further prove whether this mechanism is suitable to our system or not, the orbital energies of separate parts of BBDPB were calculated by the Gaussian 03 package. The emission property of BODIPY fluorophores can be tuned systematically by modulating the PeT process from the pendant aryl rings group to the BODIPY core, whereas, systems that are conjugatively uncoupled can possess a nonradiative PeT deactivation channel as long as the donor's HOMO is energetically located between the HOMO and LUMO of the fluorophore (Figure 7).^{35,39} According to the results of theoretical calculation,

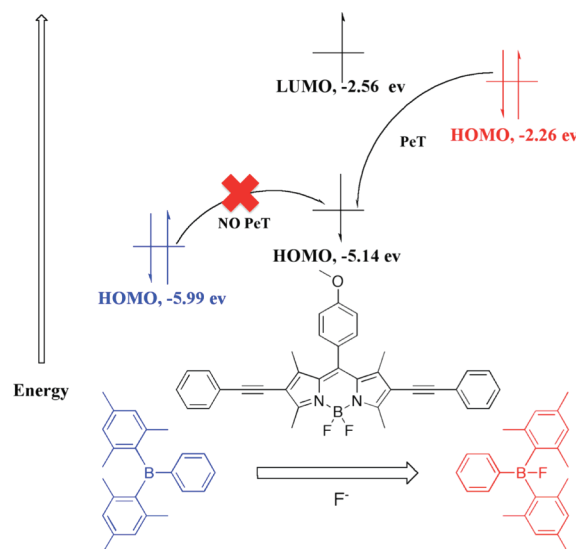


Figure 7. Frontier orbital diagram of different parts for BBDPB. Orbital energies were calculated using Gaussian 03 at the B3LYP/6-31G level.

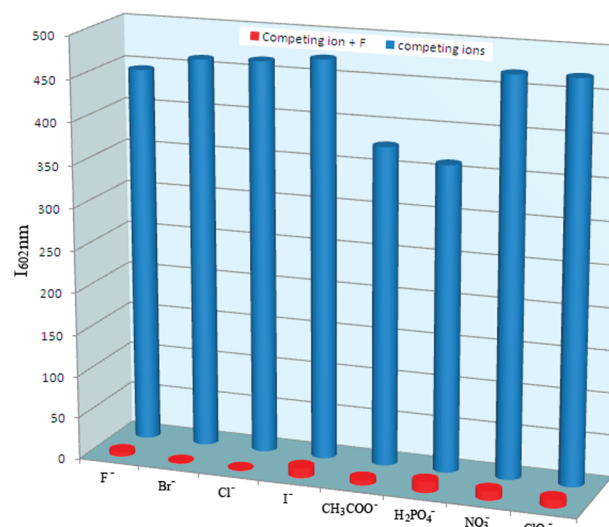


Figure 8. Photoluminescent response ($I_{602 \text{ nm}}$) of BBDPB ($2.0 \mu M$, in CH_2Cl_2) in the presence of F^- (3 equiv) and the interfering anions (7 equiv).

the HOMO energy of the Mes_2BPh group lies below the S_1 excited state of the BODIPY core, which suppressed the PeT process and made BBDPB display an orange-red emission. However, after F^- combining to the Mes_2BPh , the HOMO energy of the $\text{Mes}_2\text{BPh}-\text{F}$ group lies above the S_1 excited state of BODIPY core, which made the $\text{Mes}_2\text{BPh}-\text{F}$ group participate in the PeT process with the excited state of the fluorophore and quenched BBDPB's fluorescent emission. So, by calculating the HOMO energy for Mes_2BPh (-5.99 eV) and $\text{Mes}_2\text{BPh}-\text{F}$ (-2.26 eV) and comparing them to the values for PhBDPPh , we reason that BBDPB may be engaged in PeT after Mes_2B binding with F^- , resulting in quenching of fluorescence emission.

3.5. Selective Optical Response of BBDPB to Various Anions. For an excellent probe, high selectivity is necessary. Achieving high selectivity for anions of interest over other potentially

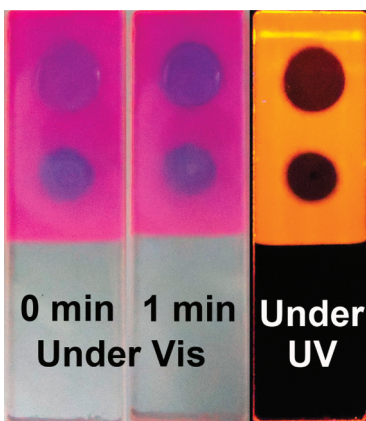


Figure 9. Photos showing phosphorescence color changes over time of the PMMA film doped with BBDPB upon placing a droplet of the CH_3CN solution containing F^- (top droplet, 0.1 mM; bottom droplet, 1 mM).

competing species is a challenge in anion probe development. Herein, the experimental results suggest that BBDPB shows high selectivity in fluorescent probes for fluoride anions. As depicted in Figure 8, only the addition of F^- results in prominent changes of luminescence intensity at $\lambda = 602 \text{ nm}$, whereas the addition of an excess of other anions (Br^- , Cl^- , I^- , H_2PO_4^- , CH_3COO^- , NO_3^- , and ClO_4^-) causes little or slight changes.

3.6. Solid-State Detection of BBDPB for F^- . The realization of solid-state detection is quite meaningful for the sensor in practical application as portable sensing devices. To fabricate the portable sensing devices, a polymethylmethacrylate (PMMA) film doped by BBDPB was obtained by spin-coating. The response of PMMA film doped with BBDPB to F^- was investigated and is shown in Figure 9. We took a droplet of a CH_3CN solution containing fluoride ions and dropped it onto the top of PMMA films doped with BBDPB. The color of area contacting with the solution changed gradually from pink to blue. Under 365 nm optical irradiation, the orange fluorescence is quenched completely. Therefore, a sensing device for F^- with excellent performance was realized.

4. CONCLUSION

In summary, we have synthesized an excellent fluorophore BBDPB based on BODIPY containing dimesitylboryl unit. The fluorophore has an intense absorption at $\lambda = 576 \text{ nm}$ with molar extinction coefficients of $\epsilon > 10^5 \text{ mol}^{-1} \text{ dm}^3 \text{ cm}^{-1}$ and displays highly efficient orange-red emission at $\lambda = 602 \text{ nm}$. This BODIPY dye can be used as a highly selective fluorescent probe for F^- anions, attributed to the modulation of the PeT process between BODIPY core and Mes_2BPh group. The F^- sensing is accompanied with the significant fluorescence quenching of the BODIPY dye and the evident color change from pink to blue detectable by the naked eyes. Finally, the solid films of the probe in PMMA also exhibited high sensitivity and rapid response to fluoride ions, which enables the realization of a practical sensing system.

■ ASSOCIATED CONTENT

5 Supporting Information. Characterization data of compounds, normalized UV-vis and PL spectroscopic of BBDPB in different solvents, and UV-vis and PL spectroscopic titrations of

BBDPB ($2 \times 10^{-6} \text{ M}$) with different anions. This material is available free of charge via the Internet at <http://pubs.acs.org>.

■ AUTHOR INFORMATION

Corresponding Author

*Fax: +86 25 8586 6396. E-mail: wei-huang@njupt.edu.cn (W.H.); iamqzhao@njupt.edu.cn (Q.Z.); yanghuiying@sutd.edu.sg (H.Y.Y.).

Author Contributions

[†]These authors contributed equally to this work.

■ ACKNOWLEDGMENT

This work was financially supported by the National Basic Research Program of China (973 Program, 2009CB930601), the National Natural Science Foundation of China (21171098, 21174064, 50803028, 20804019, and 20974046), the Natural Science Foundation of Jiangsu Province of China (BK2009427), the Natural Science Fund for Colleges and Universities in Jiangsu Province (10KJB510010), the Scientific and Technological Activities for Returned Personnel in Nanjing City (NJ209001), and Nanjing University of Posts and Telecommunications (NY208045 and NY210029). One of the authors, Y.H.Y., thanks International Design Center research grant for financial support in this work.

■ REFERENCES

- (1) Beer, P. D.; Gale, P. A. *Angew. Chem., Int. Ed.* **2001**, *40*, 486–516.
- (2) Martinez-Manez, R.; Sancenon, F. *Chem. Rev.* **2003**, *103*, 4419–4476.
- (3) Suksai, C.; Tuntulani, T. *Chem. Soc. Rev.* **2003**, *32*, 192–202.
- (4) Gale, P. A.; Garcia-Garrido, S. E.; Garric, J. *Chem. Soc. Rev.* **2008**, *37*, 151–190.
- (5) Caltagirone, C.; Gale, P. A. *Chem. Soc. Rev.* **2009**, *38*, 520–563.
- (6) Briancon, D. *Rev. Rhumat.* **1997**, *64*, 78–81.
- (7) de Silva, A. P.; Gunaratne, H. Q. N.; Gunnlaugsson, T.; Huxley, A. J. M.; McCoy, C. P.; Rademacher, J. T.; Rice, T. E. *Chem. Rev.* **1997**, *97*, 1515–1566.
- (8) Valeur, B.; Leray, I. *Coord. Chem. Rev.* **2000**, *205*, 3–40.
- (9) Gunnlaugsson, T.; Glynn, M.; Tocci, G. M.; Kruger, P. E.; Pfeffer, F. M. *Coord. Chem. Rev.* **2006**, *250*, 3094–3117.
- (10) Zhao, Q.; Li, F.; Liu, S.; Yu, M.; Liu, Z.; Yi, T.; Huang, C. *Inorg. Chem.* **2008**, *47*, 9256–9264.
- (11) Hu, R.; Feng, J.; Hu, D.; Wang, S.; Li, S.; Li, Y.; Yang, G. *Angew. Chem., Int. Ed.* **2010**, *49*, 4915–4918.
- (12) Bao, Y.; Liu, B.; Wang, H.; Tian, J.; Bai, R. *Chem. Commun.* **2011**, *47*, 3957–3959.
- (13) Loudet, A.; Burgess, K. *Chem. Rev.* **2007**, *107*, 4891–4932.
- (14) Ulrich, G.; Ziessel, R.; Harriman, A. *Angew. Chem., Int. Ed.* **2008**, *47*, 1184–1201.
- (15) Sun, H. B.; Liu, S. J.; Ma, T. C.; Song, N. N.; Zhao, Q.; Huang, W. *New J. Chem.* **2011**, *35*, 1194–1197.
- (16) Tanaka, D.; Takeda, T.; Chiba, T.; Watanabe, S.; Kido, J. *Chem. Lett.* **2007**, *36*, 262–263.
- (17) Lin, S. L.; Chan, L. H.; Lee, R. H.; Yen, M. Y.; Kuo, W. J.; Chen, C. T.; Jeng, R. J. *Adv. Mater.* **2008**, *20*, 3947–3952.
- (18) Collings, J. C.; Poon, S. Y.; Le Droumaguet, C.; Charlot, M.; Katan, C.; Palsson, L. O.; Beeby, A.; Mosely, J. A.; Kaiser, H. M.; Kaufmann, D.; Wong, W. Y.; et al. *Chem.—Eur. J.* **2009**, *15*, 198–208.
- (19) Caruso, A.; Tovar, J. D. *J. Org. Chem.* **2011**, *76*, 2227–2239.
- (20) Li, D.; Yuan, Y.; Bi, H.; Yao, D. D.; Zhao, X. J.; Tian, W. J.; Wang, Y.; Zhang, H. Y. *Inorg. Chem.* **2011**, *50*, 4825–4831.
- (21) Xu, W. J.; Liu, S. J.; Sun, H. B.; Zhao, X. Y.; Zhao, Q.; Sun, S.; Cheng, S.; Ma, T. C.; Zhou, L. X.; Huang, W. *J. Mater. Chem.* **2011**, *21*, 7572–7581.
- (22) Yang, L. X.; Bai, D. R.; Ning, W. S. *Angew. Chem., Int. Ed.* **2006**, *45*, 5475–5478.

- (23) Zhao, C. H.; Sakuda, E.; Wakamiya, A.; Yamaguchi, S. *Chem.—Eur. J.* **2009**, *15*, 10603–10612.
- (24) Xu, W. J.; Liu, S. J.; Zhao, X. Y.; Sun, S.; Cheng, S.; Ma, T. C.; Sun, H. B.; Zhao, Q.; Huang, W. *Chem.—Eur. J.* **2010**, *16*, 7125–7133.
- (25) Wade, C. R.; Broomsgrove, A. E. J.; Aldridge, S.; Gabbai, F. P. *Chem. Rev.* **2010**, *110*, 3958–3984.
- (26) Knorr, S.; Grupp, A.; Mehring, M.; Grube, G.; Effenberger, F. *J. Chem. Phys.* **1999**, *110*, 3502–3508.
- (27) Kalinowski, J.; Stampor, W.; Mezyk, J.; Cocchi, M.; Virgili, D.; Fattori, V.; Di Marco, P. *Phys. Rev. B* **2002**, *66*, 235321–235336.
- (28) Gan, J.; Chen, K. C.; Chang, C. P.; Tian, H. *Dyes Pigm.* **2003**, *57*, 21–28.
- (29) Tanaka, F.; Rujkorakarn, R.; Chosrowjan, H.; Taniguchi, S.; Mataga, N. *Chem. Phys.* **2008**, *348*, 237–241.
- (30) Xue, L.; Liu, C.; Jiang, H. *Org. Lett.* **2009**, *11*, 1655–1658.
- (31) Zhang, X.; Chi, L.; Ji, S.; Wu, Y.; Song, P.; Han, K.; Guo, H.; James, T. D.; Zhao, J. *J. Am. Chem. Soc.* **2009**, *131*, 17452–17463.
- (32) Hanaoka, K.; Muramatsu, Y.; Urano, Y.; Terai, T.; Nagano, T. *Chem.—Eur. J.* **2010**, *16*, 568–572.
- (33) Kowalczyk, T.; Lin, Z. L.; Van Voorhis, T. *J. Phys. Chem. A* **2010**, *114*, 10427–10434.
- (34) Lu, X. Y.; Zhu, W. H.; Xie, Y. S.; Li, X.; Gao, Y. A.; Li, F. Y.; Tian, H. *Chem.—Eur. J.* **2010**, *16*, 8355–8364.
- (35) Sunahara, H.; Urano, Y.; Kojima, H.; Nagano, T. *J. Am. Chem. Soc.* **2007**, *129*, 5597–5604.
- (36) Atilgan, S.; Ozdemir, T.; Akkaya, E. U. *Org. Lett.* **2008**, *10*, 4065–4067.
- (37) Liu, J. Y.; Ermilov, E. A.; Roder, B.; Ng, D. K. P. *Chem. Commun.* **2009**, *12*, 1517–1519.
- (38) Lu, H.; Zhang, S.; Liu, H.; Wang, Y.; Shen, Z.; Liu, C.; You, X. *J. Phys. Chem. A* **2009**, *113*, 14081–14086.
- (39) Bozdemir, O. A.; Guliyev, R.; Buyukcakir, O.; Selcuk, S.; Kolemen, S.; Gulseren, G.; Nalbantoglu, T.; Boyaci, H.; Akkaya, E. U. *J. Am. Chem. Soc.* **2010**, *132*, 8029–8036.
- (40) Guo, H. M.; Jing, Y. Y.; Yuan, X. L.; Ji, S. M.; Zhao, J. Z.; Li, X. H.; Kan, Y. Y. *Org. Biomol. Chem.* **2011**, *9*, 3844–3853.
- (41) Zhang, D.; Wen, Y.; Xiao, Y.; Yu, G.; Liu, Y.; Qian, X. *Chem. Commun.* **2008**, *39*, 4777–4779.
- (42) Crosby, G. A.; Demas, J. N. *J. Phys. Chem.* **1971**, *75*, 991–1024.
- (43) Frisch, M. J.; Trucks, G. W.; Schlegel, H. B.; Scuseria, G. E.; Robb, M. A.; Cheeseman, J. R.; Montgomery, J. A., Jr.; Vreven, T.; Kudin, K. N.; Burant, J. C.; Millam, J. M.; Iyengar, S. S.; Tomasi, J.; Barone, V.; Mennucci, B.; Cossi, M.; Scalmani, G.; Rega, N.; Petersson, G. A.; Nakatsuji, H.; Hada, M.; Ehara, M.; Toyota, K.; Fukuda, R.; Hasegawa, J.; Ishida, M.; Nakajima, T.; Honda, Y.; Kitao, O.; Nakai, H.; Klene, M.; Li, X.; Knox, J. E.; Hratchian, H. P.; Cross, J. B.; Bakken, V.; Adamo, C.; Jaramillo, J.; Gomperts, R.; Stratmann, R. E.; Yazayev, O.; Austin, A. J.; Cammi, R.; Pomelli, C.; Ochterski, J. W.; Ayala, P. Y.; Morokuma, K.; Voth, G. A.; Salvador, P.; Dannenberg, J. J.; Zakrzewski, V. G.; Dapprich, S.; Daniels, A. D.; Strain, M. C.; Farkas, O.; Malick, D. K.; Rabuck, A. D.; Raghavachari, K.; Foresman, J. B.; Ortiz, J. V.; Cui, Q.; Baboul, A. G.; Clifford, S.; Cioslowski, J.; Stefanov, B. B.; Liu, G.; Liashenko, A.; Piskorz, P.; Komaromi, I.; Martin, R. L.; Fox, D. J.; Keith, T.; Al-Laham, M. A.; Peng, C. Y.; Nanayakkara, A.; Challacombe, M.; Gill, P. M. W.; Johnson, B.; Chen, W.; Wong, M. W.; Gonzalez, C.; Pople, J. A. *Gaussian 03*, Revision D.01; Gaussian, Inc.: Wallingford, CT, 2004.
- (44) Lendvay, G.; Mayer, I. *Chem. Phys. Lett.* **1998**, *297*, 365–373.
- (45) Sun, Y.; Ross, N.; Zhao, S.-B.; Huszarik, K.; Jia, W.-L.; Wang, R.-Y.; Macartney, D.; Wang, S. *J. Am. Chem. Soc.* **2007**, *129*, 7510–7511.
- (46) Liu, J. Y.; Yeung, H. S.; Xu, W.; Li, X. Y.; Ng, D. K. P. *Org. Lett.* **2008**, *10*, 5421–5424.
- (47) Parab, K.; Venkatasubbaiah, K.; Jakle, F. *J. Am. Chem. Soc.* **2006**, *128*, 12879–12885.
- (48) Hudnall, T. W.; Gabbai, F. P. *J. Am. Chem. Soc.* **2007**, *129*, 11978–11986.
- (49) Cakmak, Y.; Akkaya, E. U. *Org. Lett.* **2008**, *11*, 85–88.
- (50) Huh, J. O.; Do, Y.; Lee, M. H. *Organometallics* **2008**, *27*, 1022–1025.
- (51) Meng, G.; Velayudham, S.; Smith, A.; Luck, R.; Liu, H. *Macromolecules* **2009**, *42*, 1995–2001.